Taylor & Francis
Taylor & Francis Group

RESEARCH PAPER

🔓 OPEN ACCESS | Check for updates

Gut microbiota drives structural variation of exogenous probiotics to enhance colonization

Shuaiming Jiang[a]*, Shi Huang[b]*, Zeng Zhang[a], Wenyao Ma[a], Zhe Han[a], Yuan Song[a], Dongxue Huo[a], Weipeng Cui[a], and Jiachao Zhang[a,c]

[a]School of Food Science and Engineering, Key Laboratory of Food Nutrition and Functional Food of Hainan Province, Hainan University, Haikou, China; [b]Faculty of Dentistry, The University of Hong Kong, Hong Kong, SAR, China; [c]Collaborative Innovation Center of One Health, Hainan University, Haikou, Hainan, China

ABSTRACT

Probiotics encounter colonization resistance from native gut microbiomes, affecting their effectiveness. Genetic engineering of probiotics lacks universal applicability, as gut microbiotas are highly individualized. Here, we employed probiotic *Lactiplantibacillus plantarum* HNU082 (Lp082) to test whether Lp082 gut-adapted mutants can resolve colonization resistance in a new gut environment. Relying on culture-based methods and metagenomics, two distinct evolutionary clades of Lp082 in mice gut were observed, where one clade, which acquired more mutations, exhibited a longer survival time. However, these Lp082 isolates carrying many single nucleotide variants (SNVs) still exhibited phenotypic inconsistencies, with 13 strains of enhanced acid resistance. Thus, nanopore sequencing was proposed to identify structural variations (SVs). Among them, 12 strains had the Cro/C1-type HTH DNA-binding domain insertion, which enhanced growth and reproduction under bile salt stress, thereby increasing colonization time and quantity in the gut. The gut domestication process can drive probiotics to undergo many SNVs and SVs, thereby enhancing their colonization ability, which provides new insights into the colonization mechanisms and offers an ecology-based strategy.

Introduction

Probiotic bacteria have been widely used to promote gut health, develop the immune system,[1–3] and alleviate chronic diseases.[4,5] Successful gut microbiota modulation relies on colonizing viable probiotic bacteria in the intestine.[6] Here, "colonization" refers to establishing a permanent or long-lasting (several weeks, months, or years) presence. However, the probiotic population still faces challenges in achieving sustained colonization and persistence in the gut *in vivo*. In healthy adults, probiotic bacteria colonize the gut, lasting only a few days,[7] resulting in a gradual decline in their numbers and health benefits until re-supplementation. Even in individuals with gut disorders, which favor colonization, the gut commensals often remain resilient to the establishment of exogenous probiotic strains.[8] Another important factor associated with colonization is the gut-individualized

response to probiotic bacteria, where some individuals, regardless of age (infants or adults), show no response to probiotic interventions.[9] This can be attributed to the highly individual-specificity of the human microbiome,[10,11] shaped by genetics, diet, age, geography, disease status, and intrinsic host factors.[12] Thus, developing an effective probiotic regimen must consider the individual-specific basis.

Numerous studies have explored strategies for enhancing individualized probiotic treatment,[13,14] including optimizing the type of probiotic bacteria, administration timing, and frequency, dietary, encapsulation technologies, and engineered therapies.[15] The approaches show promise for improving probiotic effectiveness. For engineered natural strain therapies, the natural *E. coli* strains isolated from mice have been genetically engineered and reintroduced to the same host, resulting

in long-term engraftment, stability, and specific functions in the mouse gut. However, challenges remain: (1) Probiotic bacteria, typically originating from fermented foods or human feces, are still considered exogenous for consumers' gut and difficult to colonize.[16] (2) Probiotic strains often exhibit multifunctional effects, making it challenging to identify specific intervention targets and perform strain engineering. (3) Off-target effects limit the use of genome editing tools, as gene transfer between engineered bacteria and gut microbiota cannot be artificially controlled.[17] Simon Carding's team found that *Bacteroides ovatus* transferred the modified genes to resident bacteria and acquired genes enabling survival in the mice gut within 72 hours, despite the biological "kill switch" that was built to prevent the microbes from surviving *in vitro*.[18,19] (4) The complex and dynamic interactions between probiotic bacteria and the unique composition of an individual's gut microbiome remain a major challenge. Thus, the approach may not completely address the colonization resistance issue and the gut-personalized environment impact on maximizing the benefits of probiotic bacteria. Therefore, there is an urgent need to develop safe and effective probiotic treatment strategies that can maximize probiotic benefits for individuals with diverse gut microbiota compositions and health conditions.

Exogenous microbial strains have to adapt and evolve within the host throughout their life cycle.[10,20] Such adaptations help these strains better compete for limited resources and interact with the host's resident microbiome.[21,22] Extensive studies proved bacterial pathogens accumulate mutations to compete with resident microbiome and host factors when entering the host intestines.[23,24] After being introduced, probiotic bacteria also reasonably undergo adaptive evolution. In our previous study, we first demonstrated that a probiotic strain, *Lactiplantibacillus plantarum* HNU082 (Lp082), rapidly acquired adaptive mutations within the gut, significantly enhanced its carbon utilization and acid tolerance.[25]

The next question is whether these *in vivo* adaptively evolved probiotic bacteria potentially provide novel opportunities to improve their colonization duration in the following gut passages. To test this hypothesis, we performed a multi-round domestication experiment (here defined as the adaptation of probiotics driven under host-associated selective pressures) to explore the colonization ability of gut-adapted Lp082 strains. Simultaneously, we utilized metagenomic sequencing technology to investigate the ecological and evolutionary impacts of gut-adapted Lp082 strains on native gut microbiota. This study provided novel insights into the generalizable and ecology-based strategy that could revolutionize personalized probiotic therapies.

Results

The divergent evolution of probiotic bacteria during intestinal domestication in mice

Divergent evolution often refers to a population of common ancestors being split into two or more groups, leading to the development of different traits under their respective selective pressures and natural selection.[26] We hypothesize that divergent evolution also profoundly occurs for probiotic strains in the gut. Therefore, we performed a multi-round domestication experiment of the probiotic bacteria Lp082 in mice. The original Lp082 (Pro00) was first introduced into the D-Lp082 group of mice for seven days and then obtained offspring isolates (Pro01) by isolating bacteria from feces. These Lp082 (Pro01) isolates were introduced into the same mouse hosts to get a 2nd-generation of gut-adapted Lp082 (Pro02). After repeating the above procedure, the 3rd-generation Lp082 (Pro03) isolates were also obtained (Figure 1(a)). After identifying the isolates, a total of 112 isolates were received across the three stages (Supplementary Figure S1a). After that, all the SNVs of each isolate were annotated and calculated (Supplementary Tables S1-S2). According to the SNVs of all isolates, the Lp082 isolates can be clustered into two distinct clades based on the number of SNVs. There were 48 isolates belonging to clade 1, accounting for 42.86%, and 64 belonging to clade 2, accounting for 57.14%. In the early stage of colonization (first two days), clade-1 isolates were dominant. However, over time, clade-2 strains, which carry more mutations, became increasingly prevalent, and by day 24, only clade-2 strains could be isolated (Figure 1(b)). Clade-1 strains had fewer mutations and were closer to the
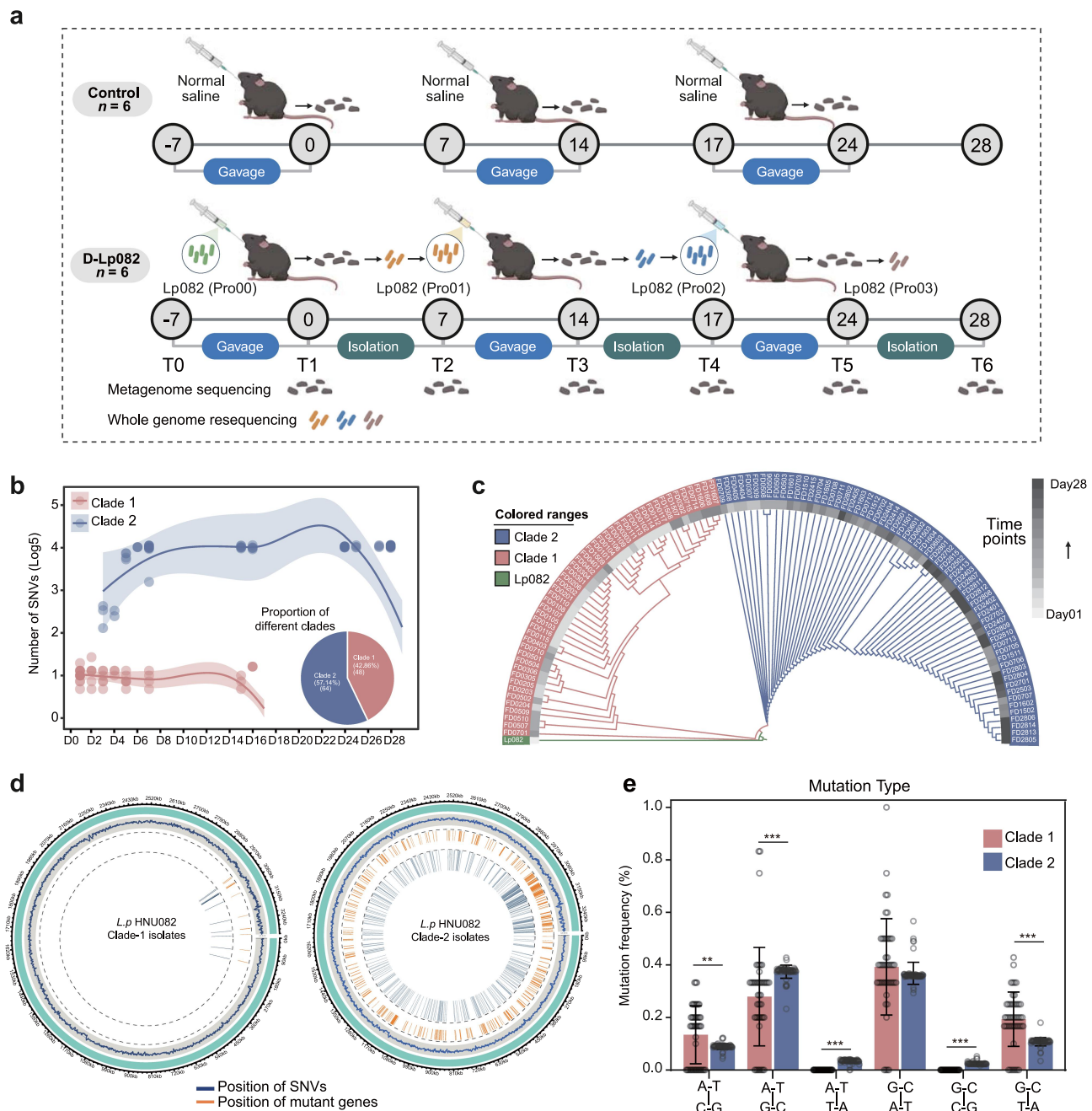
Figure 1. Experimental design and divergent evolution of probiotic bacteria. (a) Experimental design. The experiment was divided into two groups: the D-Lp082 (domestication-Lp082) and the control groups. In the D-Lp082 group, mice were fed original Lp082 (Pro00) for seven days, and then fresh feces were collected each day to obtain offspring Lp082 (Pro01) isolates by isolating bacteria from feces. Subsequently, these Lp082 (Pro01) isolates were re-administered into the same mouse hosts for seven days to obtain a 2nd-generation of gut-adapted Lp082 (Pro02). After repeating the above procedure, the 3rd-generation Lp082 (Pro03) isolates were also obtained. The whole genome of all the isolates was sequenced, and SNVs were identified by comparing them with the original Lp082. Additionally, fecal samples were collected before and after gavage at each time point for metagenomic sequencing. (b) The number of SNVs of divergent clades was observed in the fitted curve. A loess smoothing curve was fitted with a 99% confidence interval, indicated by the shaded area. The sector graph showed the number and proportion of isolates of divergent clades. There were 112 isolates, with 48 belonging to clade 1, accounting for 42.86%, and 64 belonging to clade 2, accounting for 57.14%. (c) A phylogenetic tree was constructed by the number of SNVs in the other isolates to visualize the evolutionary relationships among the isolates. Different color branches showed divergent clades, each representing a distinct clade, and the green branch presented as the root strain of Lp082. The outer gray circle represented the time of strain isolation, with the color gradually deepening from light to dark, indicating a longer period of isolation. (d) The genome circos plot illustrated the distribution of SNVs across the two clades. The outermost circle represents the reference genome of Lp082, while the second circle shows GC content as a fluctuating line. Blue lines indicated the positions of SNVs, and orange lines marked the genes in which these SNVs were located throughout the genome. (e) The mutation

original Lp082. In comparison, clade-2 strains acquired more mutations and were genetically distant from the original Lp082 (Figure 1(c)). By calculating the distances between SNV positions in different clades of isolates and performing PCoA analysis, we found that the two clades clustered separately, showing significant differences (Anosim, $p = 0.001$) (Supplementary Figure S1b). In the early stages of colonization, the proportion of clade-1 isolates was higher. Still, it was progressively eliminated during probiotic bacteria colonization. While the proportion of clade-2 isolates increased in the later stages, finally, only clade-2 strains were preserved, indicating their enhanced colonization ability and fitness advantage (Supplementary Figure S1c).

Specifically, the circular genome plot illustrated the distribution of mutations in the two clades, including the positions of SNVs and the related genes. In the genome plot of clade-2 strains, the SNVs were more densely distributed, suggesting that clade-2 strains have accumulated more mutations and also affected a greater number of genes (Figure 1(d)). Furthermore, the frequency distribution of mutation types differed between the two evolutionary clades. The mutation types were not evenly distributed in both clades. A-T to G-C and G-C to A-T substitutions occurred at relatively high frequencies, suggesting these transitions may occur more readily. Clade-1 isolates lacked A-T to T-A and G-C to C-G substitutions but exhibited a higher frequency of A-T to C-G substitutions compared to clade-2 isolates. These differences highlighted the divergence in mutational patterns between the two clades (Figure 1(e)).

Temporal evolutionary dynamics of sub-clades of Lp082 isolates

Next, examined the development of sub-clades within each clade over time and identified the occurrence of mutation sites in the two clades. Clade-2 isolates exhibited significant evolutionary distance from the original Lp082 (Figure 2(a)). Mutation E1 appeared in both sub-clades, but clade-1 isolates experienced a transient appearance of mutation E1-A-1 (Figure 2(b)). In contrast, clade-2 isolates occurred multiple parallel mutations throughout colonization (Figure 2(c)). This suggested a potential association between these preserved mutations and prolonged colonization. Parallel evolutionary genes under ramified sub-clades were also identified. In all clade-1 isolates, 14 mutant genes occurred, while in clade-2 isolates, 339 gene mutations were observed (Figure 2(d)). However, not all mutated genes were present in their respective clades. Therefore, we identified the parallel evolution genes in both clades separately and calculated the number of synonymous and non-synonymous mutations that occurred in these genes across isolates from different mice (Table S3). The results showed that clade-1 isolates had two parallel evolution genes that carried the function of transposase and putative transposase of the IS4/5 family (Figure 2(e)), while clade-2 isolates had 56 parallel evolution genes that carried more functions (Figure 2(f)). Among the 56 parallel evolution genes identified in clade-2 strains, we observed a high frequency of mutations in the Transport of potassium into the cell and NLP P60 protein gene. Potassium homeostasis is essential for bacterial survival, playing a key role in osmoregulation, pH balance, protein synthesis regulation, enzyme activation, membrane potential maintenance, and electrochemical signal transduction.[27] Additionally, the MobA MobL family protein, which also showed mutations, may be involved in plasmid transfer and horizontal gene transfer (HGT) among bacterial populations.[28] NLP P60 protein plays a widespread role in supporting the dynamics of the bacterial cell wall or bacterial growth.[29]

The synergistic adaptation of resident microbiota

The rapid within-host evolution of Lp082 was primarily driven by competition with resident gut microbiota for ecological niches. Therefore, we investigated the impact of repeated interventions

---

frequencies for different mutation types between clade-1 and clade-2 isolates were compared. Bar plots display the frequencies of base substitutions in clade-1 (red) and clade-2 (blue) strains. The x-axis represented specific base substitution types (e.g., A-T to C-G), and the y-axis indicated the relative frequency of each substitution type within each clade. Significant differences between clade-1 and clade-2 strains were indicated by *$p < 0.05$. The mutation type of A-T to C-G was higher in clade-1 isolates, while the type of A-T to T-A and G-C to C-G was higher in clade-2 isolates.
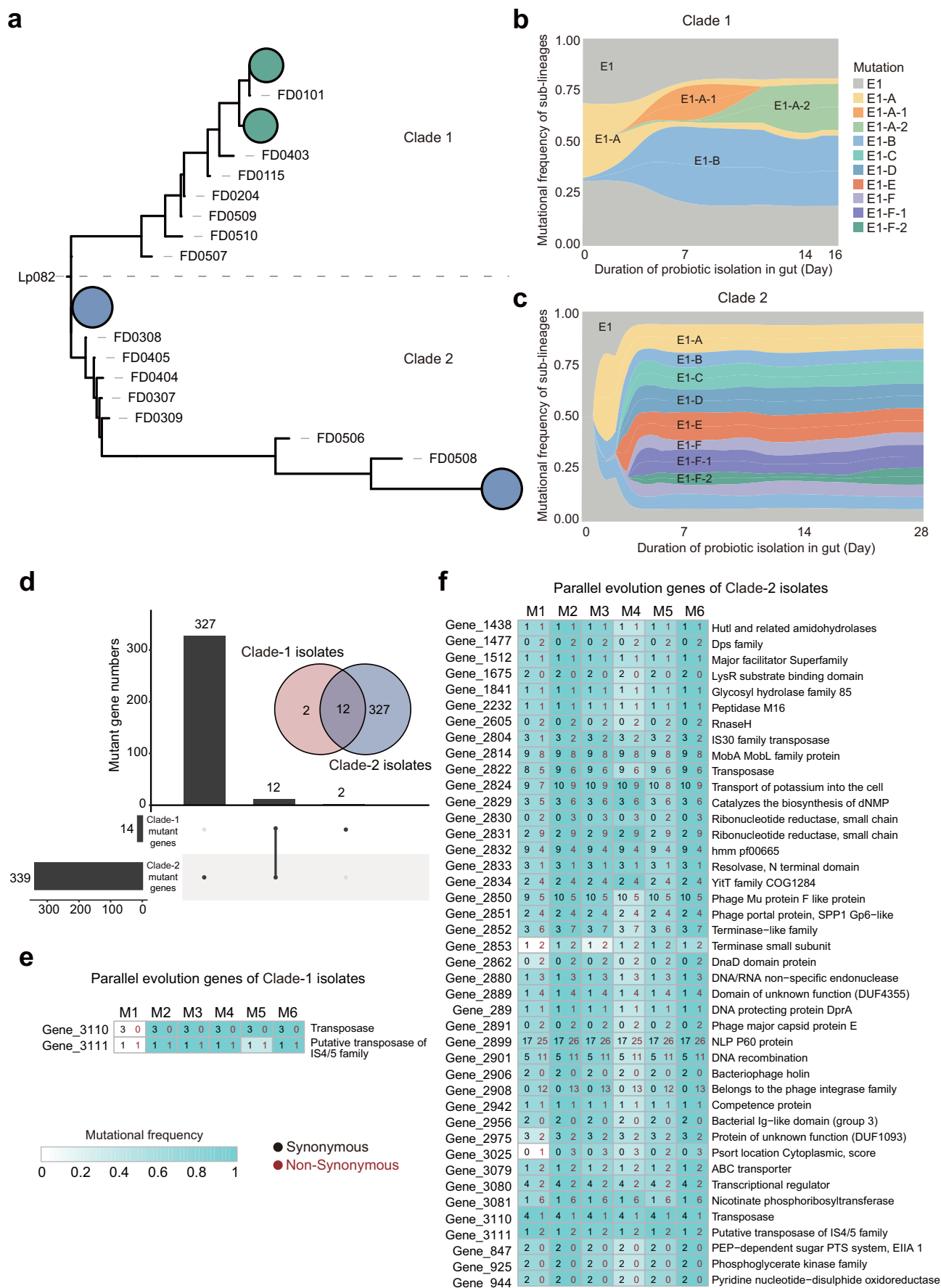
Figure 2. The parallel evolution genes of divergent clades of probiotic bacteria. (a) the simplified phylogenetic tree of two clades based on the original strain Lp082 as the root was drawn separately. (b and c) the evolutionary dynamics of the 5 branches (in

with Lp082 on the gut residents (Supplementary Tables S4). The intervention increased alpha diversity and altered the gut microbiota structure (Figure 3(a,b)). Using Spearman correlation analysis, we identified species that competed (negatively correlated) or cooperated (positively correlated) with Lp082, employing a screening threshold of r-value less than −0.3 or greater than 0.3 (Figure 3(c)). The main competitive species belonged to the genera *Lactobacillus*, *Bifidobacterium*, and *Bacteroides*. Furthermore, we identified and annotated the mutation sites of the related species in the correlation network and discovered numerous mutations in *Lactobacillus johnsonii* and the *Bacteroides* genera (Figure 3(d)), affecting critical physiological functions. According to the calculation, the number of SNVs in the local microbiota did not correlate with whether the bacterial species cooperated or competed with Lp082 throughout the intervention.

Furthermore, We computed the dN/dS values of mutant genes in these species at different time points and screened for mutant genes in these strains that showed increased dN/dS values over time (Figure 3(e)). The dN/dS value showed a continuous increase in genes of *L. johnsonii* and *Bacteroides ovatus* during the first four time points. The representative genes of *L. johnsonii* and *B. ovatus* were selected for protein functional annotation (Figure 3(f)). Gene 397 of *L. johnsonii* encoded an ABC-F family ATP-binding cassette domain-containing protein, crucial for transmembrane transport.[30] Additionally, gene 1465 of *Bacteroides ovatus* encoded HsdR family type I site-specific deoxyribonuclease, which can digest DNA to produce monodeoxynucleotides.[31] Nutrient transport and monodeoxynucleotides production are imperative for bacterial DNA replication and reproduction. It was suggested that the resident microbiota also underwent mutations in critical physiological functions while interacting with probiotic bacteria, potentially impacting long-term gut health.

Gut microbiome domesticated probiotics to drive structural variations

In all clade-2 Lp082 isolates, though many identical SNVs occurred, the strains' acid tolerance remained inconsistent. Thirteen strains exhibited higher tolerance at pH 3.0 than the original Lp082. Thus, we speculated that this phenotype difference may be due to SVs with long sequences, which cannot be identified by whole-genome resequencing. Therefore, we performed nanopore sequencing on these 13 gut-adapted Lp082 strains (Figure 4(a)). After quality control, assembly, and polish, the assembled genomes for these 13 strains were obtained (Figure 4(b)). The average nucleotide identity (ANI) of the 13 gut-adapted strains was greater than 99.7%, indicating that they were all domesticated from the original Lp082 within the gut (Figure 4(c)). The types and quantities of insertion sequence (IS) elements showed high consistency among these gut-adapted strains, but had differences compared to the original Lp082 (Figure 4(d)). The specific information on IS sequences and functional annotations of upstream and downstream genes in each strain's genome were provided (Supplementary Tables S5-S8).

Furthermore, using the original Lp082 as a reference genome, SVs annotation revealed different types and numbers of insertions, deletions, inversions and duplications varied across these 13 gut-adapted strains (Figure 4(e)). Upon detailed analysis, we further found that, when mapped to the original Lp082 sequence, most strains exhibited insertions or deletions at the same positions in

different colors) in clade 1 (b) and the 9 branches in clade 2 (c) based on mutational frequency were constructed during the probiotic colonization in the gut. (d) parallel evolutionary genes under sub-clades were also identified. The venn diagram summarized the overlap of mutant genes between the two clades. The bottom panel visualizes the mutant gene counts within each clade. The black dot indicates the number of mutated genes observed within the clade isolates, and the gray dot represents the mutant genes detected in an individual isolate from either clade. In all clade-1 isolates, 14 mutant genes occurred, while in clade-2 isolates, 339 gene mutations were observed. Bar plots showed the number of mutant genes unique to clade-1 (2 genes), unique to clade-2 (327 genes), and shared between both clades (12 genes). (e and f) parallel evolution genes of sub-clades were shown in the heatmap. Cell color and number represented the mutation frequency and the number of SNVs in the gene, respectively, of sub-clades. Cyan cells indicated the gene mutation frequency from sub-clade isolates in each mouse. The black number in each cell showed the number of synonymous mutations in the gene in each mouse, and the red number represented the number of non-synonymous mutations in the gene. (e) clade-1 isolates had two parallel evolution genes, while (f) clade-2 isolates had 56 parallel evolution genes.
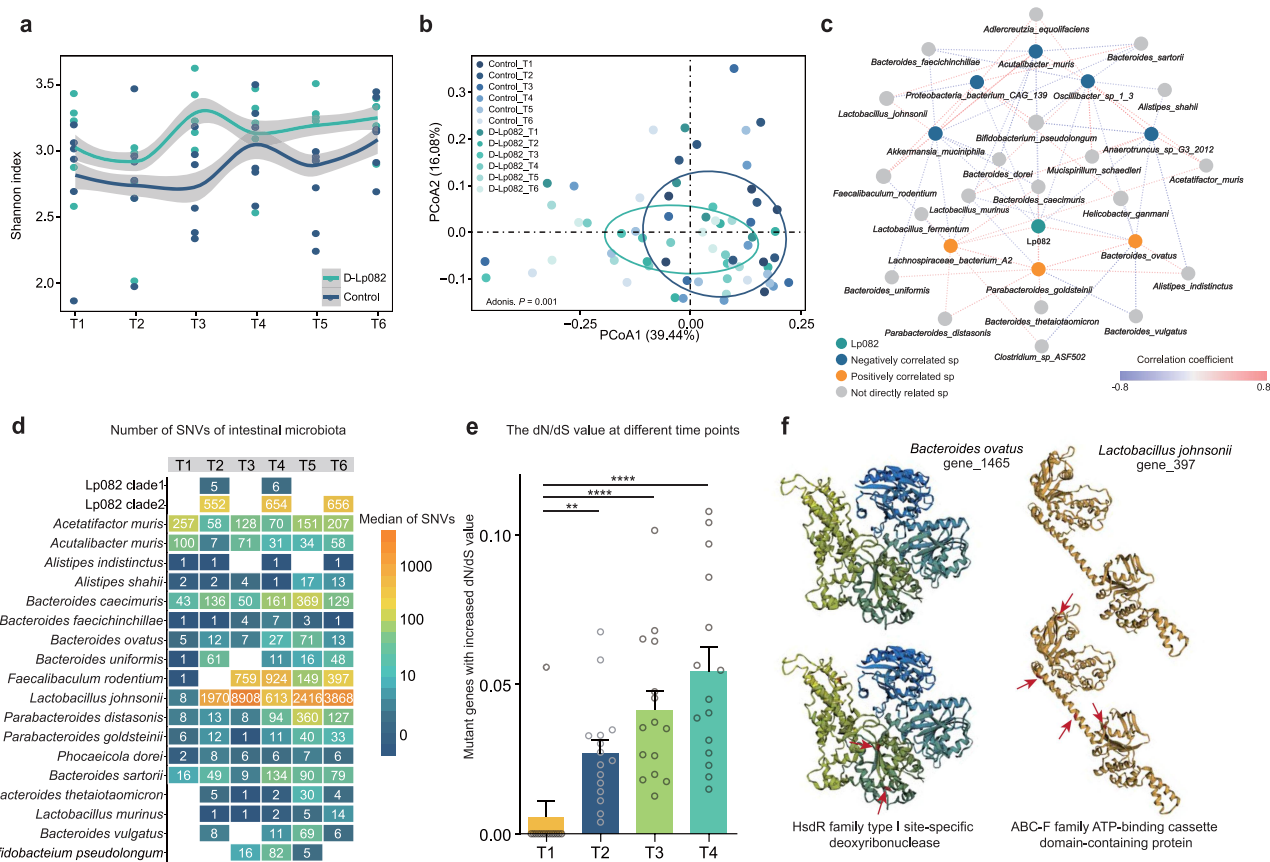
Figure 3. The response and mutations of the related species of the resident microbiome. (a) The alpha diversity of D-Lp082 and the control group was shown with the Shannon index, showing the richness and evenness within the group. (b) The shifts of microbiota structure based on Bray-Curtis distance in the control and D-Lp082 group after the probiotic engraftment were shown with Adonis. $p = 0.001$. The colored point showed the samples at distinct time points. (c) Correlation network related Lp082 in intestinal microbiota. Orange points represented the bacteria positively correlated with Lp082, while blue points represented the bacteria competing directly with Lp082. The gray points represented the species indirectly related to Lp082. The r-value threshold was 0.4. The color of the line connection between points indicated a correlation. (d) The number of mutation sites of bacteria related to Lp082 at different time points after probiotic bacteria intervention. (e) The mutant genes with increased dN/dS value in these strains at different time points. (f) The protein structure of gene 1465 of *bacteroides ovatus* and gene 397 of *L. johnsonii*. the mutation site was marked in red, and the protein conformation, as predicted by the software, did not change significantly before and after the mutation.

the reference genome (Figure 4(f)). Yet, the length of the inserted or deleted fragments varied across these gut-adapted strains, indicating the insertion or deletion of different gene segments. Additionally, the pie chart demonstrated that the proportion of insertions/deletions in these strains was inconsistent, proving that the gut-adapted strains' genomes did not simply undergo gene translocations to different positions (Figure 4(g)).

The genes involved in the four types of SVs across the 13 strains were annotated (Supplementary Figure S2). The genes involved in deletion-type and insertion-type structural variations (SVs) across the 13 gut-adapted Lp082 strains were shown. Gene functions that were inserted or

deleted in more than 80% of these strains were displayed (Figure 5(a)). The Cro/C1-type HTH DNA-binding gene underwent insertion in 12 strains, resulting in an additional Cro/C1-type HTH DNA-binding gene in each of these strains. Bacterial toxin-antitoxin (TA) systems are generally stable under normal conditions.[32,33] Still, under environmental stress (such as bile salts), the antitoxin is degraded by proteases, leading to toxin release and bacterial death.[34] The Cro/C1-type HTH DNA-binding gene can substitute for the degraded antitoxin by binding to the toxin, thus lifting the growth and proliferation limitations on the bacteria (Figure 5(b)). The gene sequences of the Toxic component of a toxin-antitoxin (TA)
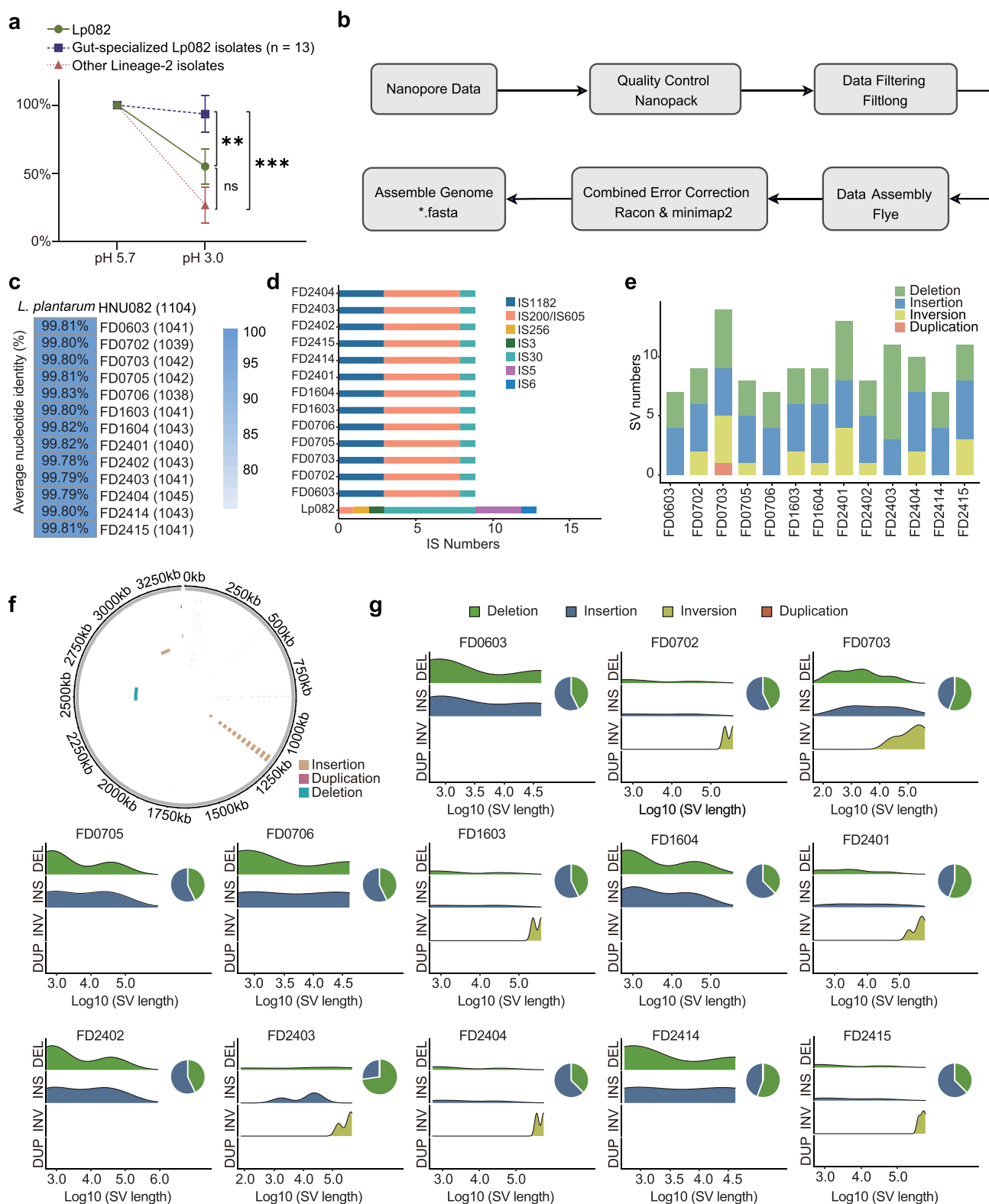
Figure 4. The long sequence structural variation annotation of the gut-adapted Lp082 isolates. (a) Results of acid tolerance experiments for each strain of clade-2 isolates showed that thirteen strains exhibited higher tolerance at pH 3.0 than the original Lp082 ($p < 0.01$). (b) The quality control, assembly, and Polish process for the nanopore sequence data of these 13 strains. (c) The average nucleotide identity (ANI) of the 13 gut-adapted strains. (d) Characterization of is insertion sequences among these gut-adapted strains. (e) SVs annotation across these 13 gut-adapted strains, including different types and numbers of insertions, deletions, inversions, and duplications. (f) Genome circle plots visualized the position of SVs occurring in 13 gut-adapted strains on the genome, with colors indicating the type of SVs. (g) SVs length distribution of different types in 13 gut-adapted strains. The pie chart demonstrates the proportion of insertions/deletions.
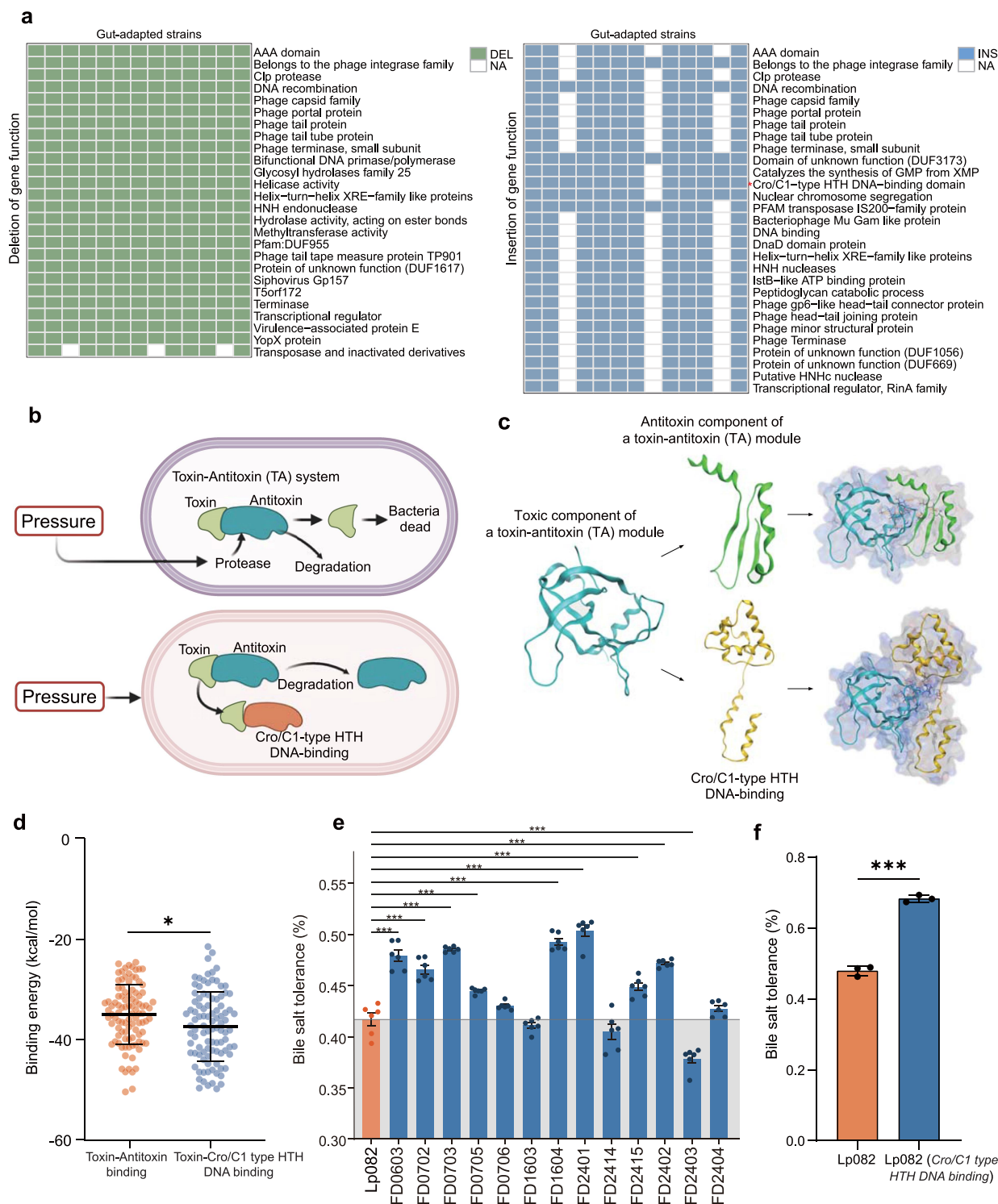
Figure 5. The long sequence structural variation annotation of the gut-adapted Lp082 isolates. (a) The genes involved in deletion-type and insertion-type structural variations (SVs) across the 13 gut-adapted Lp082 strains were shown. Gene functions that were inserted or deleted in more than 80% of these strains were displayed. Each row represented a specific gene function, and each column represented a different gut-adapted strain. Green squares (labeled DEL) indicated gene function deletions, and blue squares (labeled INS) represented inserted gene functions in the corresponding strain, white squares (NA) indicated no detected deletion. For the specific annotation, see supplementary tables S9-S12. (b) The potential functional mechanisms for the insertion gene Cro/C1-type HTH DNA-binding. (c) The protein structures of three genes, the Toxic component of a toxin-antitoxin (TA) module, the antitoxin component of a TA module, and the Cro/C1-type HTH DNA-binding protein were predicted, along with the conformations and intermolecular interactions of their two distinct protein-protein complexes. (d) Binding energies (kcal/mol) were predicted across 100 independent simulations for two interaction scenarios: (1) between the Toxic component and antitoxin component of the TA module,

module, Antitoxin component of a toxin-antitoxin (TA) module and Cro/C1-type HTH DNA-binding protein were identified from the Lp082 genome, and their corresponding protein sequences were obtained. These structures were then used to simulate protein conformations and intermolecular interactions to predict the binding conformations and structural stability of protein-protein complexes formed via two distinct binding modes (Figure 5(c)). For each interaction type, binding energies were calculated across 100 independent simulations. The results showed that both interaction modes yielded favorable docking conformations. The complex between the Toxic component and Cro/C1-type HTH DNA-binding protein exhibited lower binding energy values, indicating greater stability (Figure 5(d)). This mechanism might help gut-adapted strains resist bile salts and further enhance their colonization ability in the gut. Validation through *in vitro* experiments confirmed a significant enhancement in bile salt tolerance in the gut-adapted strains (Figure 5(e)). To further validate the functional role of the Cro/C1-type HTH DNA-binding gene, this gene was overexpressed and transformed into the original Lp082 strain. Then, the bile salt tolerance of the original Lp082 and the overexpression Lp082 strains were assessed. The results demonstrated a significantly increased survival rate under bile salt stress in the strain overexpressing the Cro/C1-type HTH DNA-binding gene ($p < 0.001$), confirming that this gene could play a critical role in enhancing Lp082's resistance to bile salt stress (Figure 5(f)).

Gut-adapted Lp082 has enhanced colonization ability and less disturbance to the gut microbial community

Then, we verified the colonization ability of these gut-adapted Lp082 strains in mice. The original and gut-adapted Lp082 were simultaneously administered orally to mice. Absolute quantification of Lp082 in the feces was performed (Figure 6(a)). The qPCR analysis showed that the gut-adapted strains had a longer colonization time and higher abundance ($p < 0.001$) compared to the original Lp082 in the fecal metagenomes (Figure 6(b)). Moreover, from the Chao1 index, we found that gut-adapted Lp082 had a different impact on the intestinal microbiota compared to the original Lp082, causing less influence to the intestinal microbial community. Specifically, the diversity and structure of the native intestinal microbiota differed between the two groups. In contrast, the Lp082-M group showed lower diversity, with no significant difference compared to the Control group (Figure 6(c)). There were no significant shifts in the overall microbial community structure (Figure 6(d)). To assess the impact of the original and gut-adapted Lp082 strain on the ecological structure of the gut microbiota in mice, we compared key ecological indicators of microbial communities between Lp082 and Lp082-M group. The results showed no significant difference in niche breadth between the two groups, indicating similar diversity in overall resource utilization within the gut microbiota (Supplementary Figure S3a). However, in the Lp082-M group, the niche overlap between Lp082 and other members of the gut microbiota was significantly reduced ($p < 0.01$), suggesting a greater degree of functional differentiation within the community (Supplementary Figure S3b). This reduced overlap may alleviate interspecies resource competition and promote ecological coexistence among community members.[9] In addition, network robustness refers to the ability of the microbial network to withstand the loss of nodes when subjected to random perturbations. Compared to the Lp082 group, the Lp082-M group exhibited significantly higher microbial robustness ($p < 0.05$), indicating that the gut community structure following intervention with the gut-adapted Lp082 was more stable and resilient in response to environmental fluctuations

and (2) between the Toxic component and the Cro/C1-type HTH DNA-binding protein. The docking energy of the Toxic component – Cro/C1-type HTH DNA-binding protein complex was significantly lower ($p < 0.05$), indicating a stronger binding affinity in this interaction. (e) The bile salt tolerance in the gut-adapted strains was verified through in vitro experiments. (f) The bile salt tolerance of the original Lp082 and the overexpression of the Cro/C1-type HTH DNA-binding gene of Lp082 strains was assessed. The survival rate of the Lp082 strain overexpressing the Cro/C1-type HTH DNA-binding gene was significantly higher than that of the original strain after 3 hours of incubation in MRS medium containing 0.3% bile salts ($p < 0.001$).
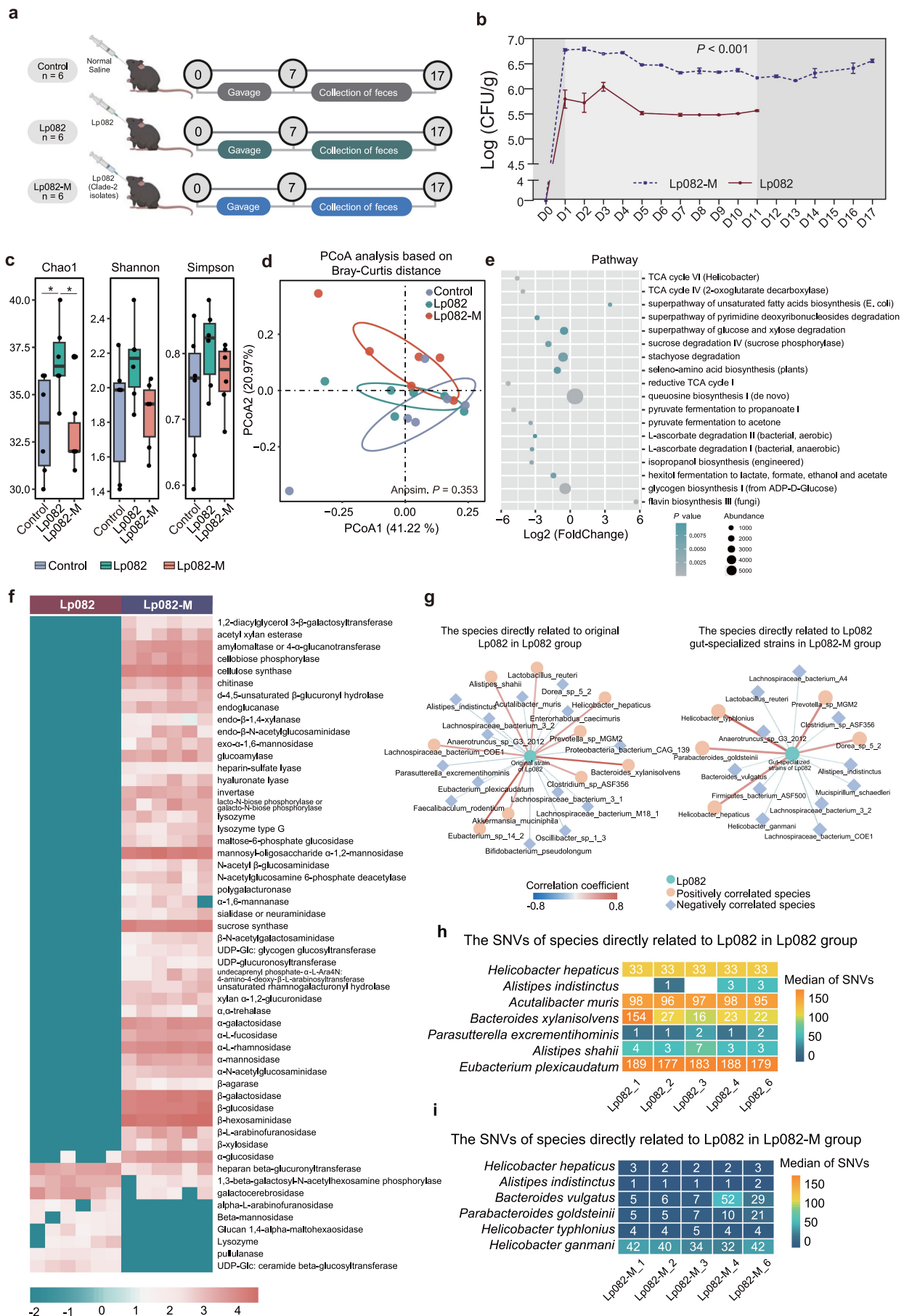
Figure 6. Comparison of colonization ability and impact on gut microbiota between gut-adapted Lp082 strains and the original Lp082 strain. (a) The colonization ability of these gut-adapted Lp082 strains in mice was verified. The original Lp082 and gut-adapted Lp082

(Supplementary Figure S3c). Taken together, these results demonstrated that gut-adapted Lp082 enhanced the stability of the intestinal microbiota, reduced interspecies competition for resources, and may facilitate its long-term adaptation and colonization within the host gut environment.

The differential metabolic pathways were implicated in pyruvate fermentation, carbohydrate degradation, and glycogen biosynthesis (Figure 6 (e)). To investigate the changes in acid composition in the fecal samples, the content of short-chain fatty acids (SCFAs) in the fecal contents of the Lp082 group and Lp082-M group was measured (Supplementary Figure S4). The results indicated that the changes in SCFA levels in fecal samples were different between the Lp082 and gut-adapted Lp082 interventions. Compared to the original strain, the gut-adapted Lp082 intervention decreased the propionate content but increased the levels of butyric acid and caproic acid. In contrast, Lp082 significantly increased the propionate content. This may be due to the fact that Lp082 and its gut-adapted Lp082 strain affect the gut microbiota differently, leading to distinct utilization of various carbohydrates, which in turn impacts the SCFA levels in the fecal samples.

Also, consumption of the gut-adapted Lp082 further enriched the carbohydrate pathway abundance in the resident gut microbes (Figure 6(f)). We further examined the resident species directly related to the Lp082 using correlation analysis and identified their strain-related SNVs in the Lp082 and Lp082-M groups. The correlation network revealed that the original Lp082 had a greater impact on the gut resident microbiota than the gut-adapted Lp082 (Figure 6(g)). After consuming the gut-adapted strain, the frequency of SNVs in the resident bacteria was relatively lower in the Lp082-M group, indicating the gut-adapted strains had a reduced ecological and evolutionary impact on the gut microbiome (Figure 6(h,i)). This lower colonization resistance may facilitate the easier colonization of the gut-adapted strain in the intestinal tract. Overall, gut-adapted probiotics not only enhance their colonization ability in the gut but also cause less ecological and evolutionary disturbance.

Discussion

Our past study characterized the within-host adaptive evolution of probiotic Lp082 and its ecological and evolutionary impact on the resident gut microbiome that was underexplored. Here, we performed a multi-round domestication experiment of probiotic bacteria Lp082 within hosts. Then we explored and verified how the gut-adapted strains enhanced gut colonization resistance and stabilized the resident gut microbiota.

The divergent evolution of probiotic bacteria within the gut may be ubiquitous yet underexplored

We observed the divergent evolution of probiotic bacteria *in vivo* based on the number of SNVs. Probiotic mutants can be divided into two clades,

---

were introduced into the Lp082 and Lp082-M (Lp082-mutant) group mice, respectively. The absolute quantification of Lp082 in the feces was performed. (b) The Lp082 content in feces after gavage by qPCR analysis during the bacteria isolation period in Lp082 and Lp082-M groups. The light gray background (from D1 to D11) indicated that there was a significant difference in Lp082 content between the two groups ($p < 0.001$), while the dark gray background indicated that the p value could not be calculated. (c) The alpha diversity of the Lp082, Lp082-M, and control groups of intestinal microbiota was shown, with the Shannon, Simpson, and Chao1 index representing the richness and evenness within the group. The Lp082 group had a higher alpha diversity than the Lp082-M group. (d) The shifts of microbiota structure between the Lp082 and Lp082-M groups after the probiotic engraftment were shown, respectively. (e) The different metabolic pathways of gut microbiota between Lp082 and Lp082-M groups were compared ($p < 0.05$). The Log2 (FoldChange) value less than 0 indicates that the metabolic pathway is less abundant in the Lp082-M group. The p values are represented by a blue-green color gradient, and the size of each dot reflects the absolute abundance of the corresponding pathway. (f) Carbohydrate pathways were also annotated. The cell color indicated the abundance of samples. Increased abundance in the Lp082-M group means the Lp082 mutants could increase the carbohydrate utilization of gut microbiota more than the original Lp082. (g) The correlation network map was directly related to the introduced strain in the Lp082 and Lp082-M groups. Correlation network related Lp082 in intestinal microbiota. Orange points represented the bacteria positively correlated with Lp082, while blue points represented the bacteria competing directly with Lp082. The r-value threshold was 0.4. The color of the line connection between points indicated a correlation. More species interacted with the original Lp082. (h and i) the number of SNVs of the species related to Lp082 and Lp082 mutants in the Lp082 and Lp082-M groups was identified separately. There were also fewer SNVs of the species interacting with the Lp082 mutants in the Lp082-M group.

where clade-2 strains acquired more SNVs and gradually replaced clade-1 Lp082. Mutations occur randomly and accumulate over time, leading to a divergence between different clades. Certain advantageous mutations become enriched in specific clades, allowing individuals with adaptive traits to survive and pass on these traits to their offspring, resulting in higher survival rates and better adaptation to the environment.[35] This principle aligns with Darwinian theory and has been observed in various organisms, including pathogens and our probiotic study. Our preliminary results found that the probiotic evolved divergently *in vivo*, with one clade acquiring more mutations and exhibiting more prolonged survival than another in the gut. Similar observations have been proved in pathogens, such as *Enterococcus gallinarum*, which diverged into independent clades due to within-host evolution. Among them, mucosally adapted strains increased translocation to and survival and facilitated the initiation of inflammation.[36] Additionally, adaptive mutants of *Staphylococcus aureus* spread throughout the entire body, and the acapsular USA300 clade of *S. aureus* demonstrated the advantages over capsular strains for colonization of nares.[37] That may be mutation accumulation, and natural selection drives evolutionary divergence in microorganisms.

This divergence provides insights into the complex interactions between probiotic bacteria and the host gut microbiome and their adaptation and colonization in the gut, And the theory of microbiota-driven adaptive evolution of probiotics may have general applicability. Our previous research has shown that two probiotics (Lp082 and *Bifidobacterium animalis* subsp. *lactis* V9) can both undergo adaptive mutations in the mouse gut and have also been observed to exhibit a trend toward divergent evolution.[38] However, such patterns of evolution were not observed in germ-free mice. Based on this, we reasonably speculated that similar microbiota-driven adaptive evolution of probiotics may also occur in the human or other mammals' gut. Moreover, due to strain-specific competition with native microbes over diverse nutrient resources, different probiotic strains may undergo comparable patterns of divergent evolution, this remains to be experimentally validated. Understanding these dynamics is crucial for optimizing probiotic properties and their beneficial effects in the gut environment.

With long fragment SVs, more fitness advantages would be gained from probiotic bacteria bypassing the gut

Our previous study confirmed that resource competition with the gut microbiota drives mutations in probiotic bacteria *in vivo*, suggesting a more competitive gut environment promoted adaptive evolution. Further, we observed that probiotic strains within the gut underwent distinct SVs landscape, including insertions and deletions of numerous genes, thus enhancing tolerance in the intestine and promoting intestinal colonization. These occurrences of SV had the potential to serve as an adaptive strategy for probiotics to improve survival and colonization efficiency in their intestines. In particular, gene fragments related to stress resistance mechanisms, such as the TA system, may confer selective advantages under stressful conditions of the intestinal environment. Thus, gut microbiota can be used to drive the evolution of probiotics to obtain the gut-adapted strains.

Gut-adapted Lp082 strain showed less disturbance to the gut microbial community

The gut-adapted Lp082 strain exhibited a reduced impact on both microbial diversity and the evolution of the native microbiota. This may be attributed to the combined effect of several factors. First, due to its enhanced tolerance to the host gut environment, the gut-adapted Lp082 likely experiences lower ecological overlap and competition, allowing it to coexist more harmoniously with resident microbes. Second, the gut-adapted Lp082 strain appeared to influence local microbial nutrient utilization, particularly in carbohydrate metabolism, potentially reducing overlap with existing metabolic pathways in the community and thus minimizing resource competition. Finally, the reduced competition exerted by the gut-adapted Lp082 strain on gut bacteria may result in weaker selective pressure, reflecting a more stable ecological behavior and contributing to the observed lower number of SNVs within gut species.

Why and how are those gut-adapted probiotic bacteria in the feces beneficial?

In this study, gut-adapted strains that have undergone intestinal adaptation demonstrated an increase in colonization ability in other mice intestinal environments without probiotic bacteria intervention before, with less disturbance to the local microbial community and their mutations, indicating that gut-adapted strains have a higher adaptability to the mice gut environments. Adaptive evolution of probiotics in the gut can enhance their abundance and survival time, indicating improved colonization capacity. This facilitated the establishment of stable microbial communities within the gut, enabling the probiotic strains to exert their beneficial effects more persistently and contribute to long-term host health. Moreover, adaptive evolution may also bring probiotics with novel functions, such as increased bile acid tolerance, thereby maintaining and enhancing their functional capabilities and competitive fitness. These changes may further influence interactions with the native gut microbiota. However, the effectiveness of probiotic bacteria varies greatly from person to person,[39] highlighting the importance of selecting appropriate gut-adapted probiotic bacteria with high adaptability and colonization ability for personalized gut health management. This research proposed a more targeted and effective approach for screening gut-adapted probiotic bacteria.

However, the intestinal environments of the human gut are complex and dynamic.[40] It is not clear whether the adaptability gained by gut-adapted strains can still be maintained in different individuals' gut environments. From a biological perspective, there are three possibilities for applying gut-adapted strains in different gut environments: (1) Gut-adapted strains may show universal adaptability in the microbial ecosystem of various hosts, then individual differences in gut microbiota will not hinder the efficiency. Therefore, gut-adapted strains would be used for general interventions. (2) If the adaptability of gut-adapted strains is only targeted towards specific gut environments, i.e., group adaptability. In this case, the characteristics of the individual gut environment should need to be acquired and controlled in advance, then individuals were classified into different groups, thus achieving the development of therapies based on the grouped microbiota gut types. (3) In contrast, if the application of gut-adapted strains is highly host-specific, personalized interventions for each individual must be designed truly. In this study, we found that the gut-adapted strains exhibited enhanced colonization ability (both in terms of survival rate and duration) when introduced to new mice. This suggested that these strains retained their adaptive traits in terms of colonization ability, even within a similar but non-identical gut environment. Therefore, we propose that this observed adaptability may reflect either a form of group-level "universal adaptability" or host-specific, personalized adaptability in certain functional aspects. This finding highlights the potential need for future probiotic applications to be tailored with personalized (group personalized or individual personalized) strategies to achieve optimal effectiveness across different hosts.

Functional characteristics are strongly tied to the symbiotic relationship different hosts maintain. As long as the strain can support its acquired shape, it can achieve universal colonization in the microbial ecosystem of distinct hosts. For example, Clade VI strains of *Lactobacillus reuteri* exhibit elevated fitness in chickens even if isolated from humans.[41] At the same time, *Yersinia pestis* enables switching hosts with just a few horizontally acquired traits.[42] Therefore, it is reasonable to believe that gut-adapted strains after domestication in gut environments may exhibit better adaptability and have more universal applications. However, these hypotheses need further research to verify the scope of gut-adapted probiotic bacteria and their feasibility as a treatment strategy. Nonetheless, this finding provides new opportunities for gut-adapted probiotic bacteria as a potential treatment option for people who do not respond to probiotic bacteria or with specific medical conditions.

Conclusions

Collectively, we utilized a combination of traditional bacterial isolation and culture methods and metagenomics technology to characterize the divergent evolution of probiotic bacteria in the gut and identify gut-adapted strains that exhibited

enhanced adaptability and colonization ability in the gut. The gut domestication process can drive probiotics to undergo many SNVs and SVs, thereby improving their prolonged colonization ability and stable native microbiota structure in the gut. These findings provided new insights into the colonization mechanisms of probiotic bacteria and offered an ecology-based strategy for developing personalized probiotic therapy using *in vivo* models.

Methods

The study subjects and experimental design

We performed a multi-round domestication experiment to explore the evolution law of the probiotic in mice. Probiotic bacteria Lp082 was used as an experimental object. Lp082 was isolated from Hainan Yucha, a traditional fermented food,[43] and had specific functions, including preventing hyperlipidemia and regulating neurotransmitter secretion disorder.[44,45]

The mice (C57BL/6J, 10 weeks, Shanghai Slack Experimental Animal Co., Ltd., China) were divided into two groups, the Control group ($n = 6$) and D-Lp082 (Domestication-Lp082) group ($n = 6$) were kept on a 12-hour light/12-hour dark cycle with single cage feeding. The feeding temperature was $25 \pm 2°C$, with the humidity was $55 \pm 5\%$. The autoclaved cushion, water, and feed were changed once a day. The SPF regular feed was purchased from Jiangsu Synergy Pharmaceutical Bioengineering Co., Ltd., China, which consisted of corn, wheat, imported fish meal, chicken meal, soybean meal, and soybean oil, supplemented with essential amino acids, vitamins, and minerals. The Ethics Committee of Hainan University, China, approved the experimental animal protocols (No. HNUAUCC-2021-00041). First, about 10^8 CFU/g original Lp082 (Pro00) with the fodder was introduced to the mice of the D-Lp082 group each day for seven days by gavage. Then, fresh feces from mice were collected daily to obtain offspring Lp082 (Pro01) isolates until no colonies were found. Next, Lp082 (Pro01) was reintroduced to its hosts for seven days. The isolation operation was then deployed to obtain the 2nd-generation Lp082 (Pro02) isolates. After repeating the above procedure, the 3rd-generation Lp082 (Pro03) isolates were also obtained. The Control-group mice received oral administration of saline. Finally, probiotic Lp082 isolates were collected for whole genome resequencing, and the fecal samples were conducted with metagenomic sequencing.

The colonization ability of gut-adapted Lp082-carrying SVs was evaluated through an *in vivo* verification experiment. The original Lp082 and gut-adapted Lp082 were introduced into the Lp082 and Lp082-M (Lp082-Mutant) group mice, respectively. The Control group received oral administration of saline. Then, the Lp082 content in the fecal samples of the mice was quantified using qPCR, and metagenomic sequencing of the fecal samples was performed to assess the impact of the gut-adapted strains on the gut microbiota compared to the Lp082.

Isolation and confirmation of the ingested probiotic strain (Lp082) in the feces

After stopping gavage, fresh fecal samples were collected daily for isolation of Lp082. The method for isolating and identifying Lp082 from feces has been established in previous research.[25] Fresh feces were collected and diluted with 0.85% sterilized normal saline after mixing. Then, the mixture was diluted ten times to different concentrations and coated on an MRS medium plate with 50 μL 1280 μg/mL vancomycin solution and norfloxacin solution, respectively. After morphological identification, the single cultured colony was selected as the Lp082 candidates and cultured in a liquid MRS medium. After centrifugation to obtain the bacterial cells, TE (Tris – EDTA) buffer was added, followed by DNA extraction. Then, the DNA was amplified with specific primers (forward: 5'-GCCTTGAACTTTGTGCCTGTC-3'; reverse: 5'-GGCTTTGCCTGTTGATGCTTA-3'). The amplification was carried out in a 20 μL reaction system with the following PCR program: pre-denaturation at 94°C for 5 minutes, followed by 26 cycles of denaturation at 94°C for 1 minute, annealing at 62°C for 45 seconds, extension at 72°C for 20 seconds, and a final extension at 72°C for 10 minutes. The resulting amplification products were analyzed by agarose gel electrophoresis, and the one with clear bands at 269 bp was the Lp082 isolates.

Whole genome sequencing of Lp082 isolates and data quality control

After the DNA of a single bacteria was extracted and detected, a total amount of 0.2 μg DNA per sample was used as input material for the DNA library preparations. The NEB Next® Ultra™ DNA Library Prep Kit for Illumina (NEB, USA) generated the sequence library. Specifically, DNA was randomly interrupted by a Covaris ultrasonic crusher, then by repairing the terminal, adding A tail and sequencing joint, purification, PCR amplification, etc. The whole library was then prepared. After the library passed the test, the Illumina high-throughput sequencing platform NovaSeq 6000 was used for sequencing. Next, the raw sequenced reads (NCBI Accession Number: PRJNA934833 and PRJNA1186832) were performed with primary quality control using Fastp (v0.19.7).[46] The paired reads contained adapter contamination. 10% of bases are uncertain, or the proportion of low quality (Phred quality < 5) bases is over 50% would be discarded. FastANI (v1.3.1) (https://github.com/ParBLiSS/FastANI.) was used to calculate the average nucleotide identity between the isolated strains and the original Lp082,[47] ensuring isolates were evolved from Lp082 (Supplementary Tables S1).

SNV calling and phylogenetic analysis of probiotic mutants

To count the mutation sites of isolates and construct the phylogenetic tree, we annotated the mutation sites using inStrain (v1.0.0).[48] First, the genomic function information of the strain was obtained by Prodigal (v2.6.3).[49] Meanwhile, the reference database of the original Lp082 genome was built by Bowtie2,[50] and the bam file was obtained by mapping the reads of single bacteria resequencing. Finally, InStrain (https://github.com/MrOlm/inStrain) was executed to get the SNVs of each sample. The concrete parameters include inStrain profile *.sorted.bam *.fa -c 100 -f 0.49 -o *.profile -p -g ref_genes.fna.[48] In particular, the sample with the ANI of reads and reference genomes less than 95% will be abandoned. As for the construction of the phylogenetic tree, the mutation sites of all isolates were spliced, and the evolutionary distance was calculated by the neighbor-joining method to assess the similarity between sequences by MEGA-X software.[51] After that, the evolutionary tree file was generated and beautified with iTOL software (v 6.5.8).[52]

Identification of the genes with parallel evolution from divergent clades

Parallel evolutionary genes were initially defined as isolates with a common ancestral strain in different hosts with multiple mutations in the same gene to adapt to the environment. Specifically, a functional gene that occurred more than one mutation within the 2000 bp region of this gene across individuals will be considered a parallel evolutionary gene.[20,25] This study identified two parallel evolutionary genes in clade-1 isolates, while 56 were identified in clade-2 isolates.

Nanopore sequencing and SVs annotation of gut-adapted Lp082 strains

After DNA extraction of 13 gut-adapted Lp082 strains and verification of sample concentration, libraries were constructed using the PromethION platform. Following library quality control, Nanopore sequencing was performed.[53] The obtained electrical signal data were decoded into bases using a Recurrent Neural Network (RNN) algorithm, converting them into raw sequencing reads. Then, after data control using NanoPack (v1.42.0),[54] the ONT reads shorter than 2000 bp were filtered using Filtlong (v0.2.1) (https://github.com/rrwick/Filtlong). The filtered sequences were then assembled using Flye (v2.9.2),[55] and the final genome assembly was polished three times using a combination of Racon (v1.5.0)[56] and minimap2 (v2.26-r1175)[57] to obtain the complete genome. Gene function annotation was performed using Prodigal.[58] MUM&Co (v4) was used to detect genome-wide structural variations (SVs) in these gut-adapted Lp082 strains, including insertions, deletions, tandem duplications, inversions, and translocations.[59] ISEScan (v17.2.3) was employed to identify insertion sequence elements.[60]

Quantification of Lp082 in the intestinal tract by qPCR analysis

After stopping gavage, daily fecal samples of mice were collected to quantify the microbial biomass of probiotic Lp082 in feces using real-time quantitative PCR. After extracting and purifying fecal DNA as a template, the PCR amplification and detection were carried out using Lp082 specific primers on the CFX Connect Real-Time PCR instrument (Bio-Rad) with FastStart Essential DNA Green Master (Roche). Forward primer A7F (5'-GCCTTGAACTTTGTGCCTGTC-3') and the reverse primer A7R (5′- GGCTTTGCCTG TTGATGCTTA-3′). In addition, the genomic DNA of Lp082 was diluted to make a standard curve after the concentration was detected by NanoDrop Microvolume Spectrophotometers.[61] Specific settings for PCR were as follows: 95°C for 30 s; 95°C for 10 s, 60°C for 30 s, and 72°C for 30 s; repeated 39 more times. Slowly heated from 60°C to 95°C, the signal strength was detected for every 0.5°C increase in temperature, and then the melt curve was obtained by continuous fluorescence acquisition. Each sample was run in triplicate, and the average Cq value of each sample was normalized and converted to the copy number according to the standard curve.

Metagenomic DNA extraction and shotgun metagenomic sequencing and data quality control

The QIAamp® DNA Stool Mini Kit (Qiagen, Hilden, Germany) was used for metagenomic DNA extraction from fecal samples. Analysis of purity and integrity of DNA was evaluated by 0.8% agarose gel electrophoresis. Specifically, the purity of DNA was detected based on the ratio of OD 260/280 by Nanodrop,[61] and Qubit® DNA Assay Kit accurately quantified the concentration of DNA in Qubit® 3.0 Fluorometer (Invitrogen, USA).[62] All DNA samples were sequenced by Illumina HiSeq 2500 instrument in the Novogene Company (Beijing, China). Genomic DNA was fragmented by sonication to a size of 350 bp. The DNA fragments were sequenced after end-polished, A-tailed, and ligated with the full-length

adapter. The data quality control of the raw reads was performed based on Fastp.[46]

Identification of metagenomic species, microbial functional genes, and metabolic pathways

The species abundance was annotated by MetaPhlAn3 software.[63] Functional annotations were performed using HUMAnN3 (v3.0.1) software.[63] More specifically, Gene families were identified using DIAMOND (v2.0.15) with the UniRef90 database,[64] and Metabolic pathways were annotated by the MetaCyc database. Carbohydrate enzymes of the metagenomic sequence data were annotated using dbCAN2 (v3.0.6).[65] Briefly, the reads were assembled into contigs using MEGAHIT (v1.2.9).[66] After converting the nucleic acid sequence of contigs into a protein sequence file by Metagenemark, DIAMOND quickly aligned it to the CAZyme database to get carbohydrate annotation results. The abundance of each carbohydrate function in each sample was obtained by comparing the metagenomic sequencing reads with the genes annotated to carbohydrate function by Bowtie2.[50]

Co-evolution analysis based on shotgun metagenomic sequencing data of fecal samples

Based on the correlation between strain Lp082 and gut resident microorganisms, we employed inStrain software[48] to annotate the mutation sites for a wide array of gut microbiota. We reason that the mutation sites identified from native microbiota correlated with Lp082 in abundance at the baseline should be considered the genetic background for identifying adaptive SNVs during and after probiotic ingestion. Namely, we created a reference genome database with the representative genome of 19 microbial species ecologically related to Lp082 from the NCBI database. Then, the metagenomic sequencing reads of each sample were aligned against this reference database to identify adaptive SNVs. After removing the background mutation according to the baseline samples, the adaptive SNV profiles of the native intestinal microbes caused by probiotic intake were obtained.

Determination of short-chain fatty acids (SCFAs) in feces

The content of SCFAs in the fecal contents of the Lp082 group and Lp082-M group was measured.[67] After lyophilizing the fecal samples, 50 mg was weighed and added to a 2 mL EP tube. 500 μL of saturated NaCl solution was added, and the mixture was incubated for 30 minutes before homogenization. Then, 20 μL of sulfuric acid was added to the homogenized sample for acidification, followed by vortexing for 30 seconds. Next, 800 μL of ether was added, and the mixture was vortexed for 30 seconds before incubating for 30 minutes. The extraction process was performed in a fume hood. The suspension was centrifuged at 14,000 rpm for 15 minutes, and the supernatant was transferred to a 2 mL EP tube containing 0.25 g anhydrous sodium sulfate. After a second centrifugation, the supernatant was transferred to a headspace vial for analysis. Finally, the SCFA content was analyzed using a gas chromatography-mass spectrometry (GC-MS) system (Agilent 7890, USA).

Experimental characterization of phenotypic changes associated with SNVs in probiotic Lp082

We verified the potential phenotypic changes of the strains carrying SNVs *in vitro*, including acid and bile salt tolerance. Cryopreserved strains were activated for verification experiments. Corresponding cryopreservation tubes at −80°C were taken out. Then, the bacterial liquid was drawn out to a sterilized MRS medium tube and cultured in a 37°C constant temperature incubator for 48 hours. After the bacterial liquid was shaken evenly, 100 μL suspension was drawn and transferred in a new sterilized MRS medium tube for growth.

The MRS medium with pH values adjusted to 5.7 and 3.0 was used to verify the acid tolerance. The pH value of the culture medium was adjusted by 1 mol/L HCl solution. Following this, the 2% inoculum of activated mutant strains and the original Lp082 strain was inoculated in sterilized medium tubes of different pH values, recorded as 0 h, and the tubes were cultured in 37°C incubators for 3 h. Finally, the colonies of 0 h and 3 h were obtained by diluting and coating the culture medium to the culture plate, and the survival rate was calculated.

The MRS medium, supplemented with bile salts to a final concentration of 0.3%, was used to verify bile salt tolerance. Following this, the 2% inoculum of activated gut-adapted Lp082 strains and the original Lp082 strain was inoculated in sterilized medium tubes containing bile salts, recorded as 0 h, and the tubes were cultured in 37°C incubators for 3 h. Finally, the colonies of 0 h and 3 h were obtained by diluting and coating the culture medium to the culture plate, and the survival rate was calculated.

Overexpression of Cro/C1-type HTH DNA-binding gene via plasmid electroporation

To induce overexpression of the *Cro/C1-type HTH DNA-binding* gene in the original Lp082 strain, the P23 promoter and open reading frame·(ORF) of the gene were amplified and cloned into the pLH01 vector digested with NheI using In-Fusion cloning.[68] The resulting recombinant plasmid was subsequently introduced into Lp082 via electroporation. The successful integration was confirmed by forming colonies on MRS agar plates supplemented with chloramphenicol, which were selected in subsequent experiments.

To facilitate the electroporation of Lp082, a 2 mL culture of Lp082 grown for 24 hours was introduced into 100 mL of MRS broth supplemented with 0.2 M sucrose and 3% glycine. This was followed by incubation at 37°C in a constant-temperature incubator until the culture reached an optimal density (OD_{600} = 0.4–0.6). After centrifugation, the bacterial cells were washed twice with 1 mM $MgCl_2$, followed by a final wash with an electroporation buffer composed of 952 mM sucrose and 3.5 mM $MgCl_2$. The cells were then resuspended in the electroporation buffer. Subsequently, 60 μL of the resuspended cells were mixed with 200 ng pLH01 plasmid and transferred into a 2 mm electroporation cuvette. The GenePulser Xcell system (Bio-Rad, USA) was employed to carry out the electroporation under the following conditions: 2.1 kV voltage, 200 Ω resistance, and 25 μF capacitance. Then, 1 mL of recovery medium (MRS broth supplemented with 0.5 M sucrose and 0.1 M $MgCl_2$) was added into the cuvette, and the mixture was transferred to a sterile centrifuge tube for a 3-hour phenotypic recovery at

37°C. After transformation, the bacterial cells were plated onto MRS agar plates containing 10 μg/mL chloramphenicol and incubated in a 37°C constant-temperature incubator. The colonies were confirmed successful integration.

Quantification and statistical analysis

All statistical analyses were performed using R software (v4.0.3). Spearman correlation analysis was constructed by the "psych" package, and the visualization of the network diagram was realized in Cytoscape (v3.7.1) software.[69] The genomic Circos plot used to annotate the SNVs was drawn with the "circlize" package.[70] The fitted curve and boxplot were constructed by the "ggplot2" package.[71] The heatmap was drawn using by "pheatmap" package.[72] Alpha and Beta diversity were initially calculated on the species taxonomy level. The "vegan" package calculated the Bray-Curtis distance between groups.[73] CLR transformation of the relative abundance was performed by the "zcomposition" package.[74] Niche breadth and niche overlap were calculated using the "spaa" package,[75] while robustness was calculated following the methodology of Yuan et al.[76] Wilcoxon rank-sum tests were used to test significant differences at $p < 0.05$ between the two groups. The significance of the differences among the three groups was analyzed using the Kruskal-Wallis test, and the Dunn test was used for post hoc pairwise comparisons. Statistical significance, strong significance, and very strong significance were considered for $*p < 0.05$, $**p < 0.01$, and $***p < 0.001$, respectively. Phylogenetic tree construction and beautification were carried out through MEGA-X and iTOL software.[51,52] Protein structural predictions were carried out using the Phyre2 software.[77] The experimental design diagram was created using BioRender (https://www.biorender.com/). The prediction of protein-protein conformations and intermolecular interactions was performed using the Molecular Operating Environment (MOE) software.[78]

Author contributions

CRediT: **Shuaiming Jiang:** Formal analysis, Investigation, Validation, Visualization, Writing – original draft; **Shi Huang:** Writing – original draft, Writing – review & editing; **Zeng Zhang:** Formal analysis, Investigation, Visualization; **Wenyao Ma:** Investigation, Validation; **Zhe Han:** Validation, Visualization; **Yuan Song:** Visualization; **Dongxue Huo:** Validation; **Weipeng Cui:** Investigation; **Jiachao Zhang:** Conceptualization, Funding acquisition, Supervision, Writing – original draft, Writing – review & editing.

Disclosure statement

No potential conflict of interest was reported by the author(s).

Funding

CRediT authorship contribution statement

Conceptualization, J.C.Z.; Investigation, S.M.J., Z.Z., W.Y.M., and W.P.C.; Validation, S.M.J., Z.H., W.Y.M., and D.X.H.; Formal analysis, S.M.J., Y.S.and Z.Z.; Visualization, S.M.J., Z. Z., Z.H. and Y.S.; Writing – original draft, S.M.J., J.C.Z. and S. H.; Writing – review & editing, J.C.Z. and S.H.; Funding acquisition, J.C.Z.; supervision, J.C.Z.

Data availability statement

The sequence data have been deposited in the NCBI database, including genome resequencing (https://www.ncbi.nlm.nih.gov/bioproject/?term=PRJNA1186832.) and metagenomic sequencing data (https://www.ncbi.nlm.nih.gov/bioproject/?term=PRJNA934833).

Ethics approval and consent to participate

The Ethics Committee of Hainan University, China, approved the experimental animal protocols (No. HNUAUCC-2021-00041).

References

1. Galdeano CM, Perdigon G. The probiotic bacterium lactobacillus casei induces activation of the gut mucosal immune system through innate immunity. Clin Vaccine Immunol. 2006;13(2):219–226. doi: 10.1128/CVI.13.2.219-226.2006.
2. Henrick BM, Rodriguez L, Lakshmikanth T, Pou C, Henckel E, Arzoomand A, Olin A, Wang J, Mikes J, Tan Z, et al. Bifidobacteria-mediated immune system imprinting early in life. Cell. 2021;184(15):3884–3898. e11. doi: 10.1016/j.cell.2021.05.030.

3. Ashraf R, Shah NP. Immune system stimulation by probiotic microorganisms. Crit Rev Food Sci Nutr. 2014;54(7):938–956. doi: 10.1080/10408398.2011. 619671.

4. Ejtahed HS, Mohtadi-Nia J, Homayouni-Rad A, Niafar M, Asghari-Jafarabadi M, Mofid V. Probiotic yogurt improves antioxidant status in type 2 diabetic patients. Nutrition. 2012;28(5):539–543. doi:10.1016/j.nut.2011. 08.013.

5. Luoto R, Kalliomäki M, Laitinen K, Isolauri E. The impact of perinatal probiotic intervention on the development of overweight and obesity: follow-up study from birth to 10 years. Int J Obes. 2010;34(10):1531–1537. doi:10.1038/ijo.2010.50.

6. Wang X, Zhang P, Zhang X. Probiotics regulate gut microbiota: an effective method to improve immunity. Oxycedrus Needles Berries Mol. 2021;26(19):6076. doi: 10.3390/molecules26196076.

7. Zmora N, Zilberman-Schapira G, Suez J, Mor U, Dori-Bachash M, Bashiardes S, Kotler E, Zur M, Regev-Lehavi D, Brik RB, et al. Personalized gut mucosal colonization resistance to empiric probiotics is associated with unique host and microbiome features. Cell. 2018;174(6):1388–1405.e21. doi: 10.1016/j.cell. 2018.08.041.

8. Gibson MK, Pesesky MW, Dantas G. The yin and yang of bacterial resilience in the human gut microbiota. J Mol Biol. 2014;426(23):3866–3876. doi: 10.1016/j.jmb. 2014.05.029.

9. Ojima MN, Yoshida K, Sakanaka M, Jiang L, Odamaki T, Katayama T. Ecological and molecular perspectives on responders and non-responders to probiotics and prebiotics. Curr Opin In Biotechnol. 2022;73:108–120. doi: 10.1016/j.copbio.2021.06.023.

10. Schloissnig S, Arumugam M, Sunagawa S, Mitreva M, Tap J, Zhu A, Waller A, Mende DR, Kultima JR, Martin J, et al. Genomic variation landscape of the human gut microbiome. Nature. 2013;493(7430):45–50. doi: 10. 1038/nature11711.

11. Ferreiro A, Dantas G, Ciorba MA. Insights into how probiotics colonize the healthy human gut. Gastroenterology. 2019;156(3):820–822. doi:10.1053/j. gastro.2019.01.022.

12. Rothschild D, Weissbrod O, Barkan E, Kurilshikov A, Korem T, Zeevi D, Costea PI, Godneva A, Kalka IN, Bar N. Environment dominates over host genetics in shaping human gut microbiota. Nature. 2018;555 (7695):210–215. doi:10.1038/nature25973.

13. Kort R. Personalized therapy with probiotics from the host by TripleA. Trends Biotechnol. 2014;32(6):291–293. doi: 10.1016/j.tibtech.2014.04.002.

14. Singh TP, Natraj BH. Next-generation probiotics: a promising approach towards designing personalized medicine. Crit Rev Microbiol. 2021;47(4):479–498. doi: 10.1080/1040841X.2021.1902940.

15. Russell BJ, Brown SD, Siguenza N, Mai I, Saran AR, Lingaraju A, Maissy ES, Dantas Machado AC, Pinto AFM, Sanchez C, et al. Intestinal transgene delivery with native E. coli chassis allows persistent physiological changes. Cell. 2022;185(17):3263–3277. doi: 10. 1016/j.cell.2022.06.050.

16. Zommiti M, Feuilloley MGJ, Connil N. Update of probiotics in human world: a nonstop source of benefactions till the end of time. Microorganisms. 2020;8 (12):1907. doi: 10.3390/microorganisms8121907.

17. Fruman DA, O'Brien S. Cancer: a targeted treatment with off-target risks. Nature. 2017;542(7642):424–425. doi:10.1038/nature21504.

18. Reardon S. Genetically modified bacteria enlisted in fight against disease. Nature. 2018;558(7711):497–498. doi:10.1038/d41586-018-05476-4.

19. Wegmann U, Carvalho AL, Stocks M, Carding SR. Use of genetically modified bacteria for drug delivery in humans: revisiting the safety aspect. Sci Rep. 2017;7 (1):2294. doi:10.1038/s41598-017-02591-6.

20. Zhao S, Lieberman TD, Poyet M, Kauffman KM, Gibbons SM, Groussin M, Xavier RJ, Alm EJ. Adaptive evolution within gut microbiomes of healthy people. Cell Host Microbe. 2019;25(5):656–667. doi: 10. 1016/j.chom.2019.03.007.

21. Suerbaum S, Josenhans C. Helicobacter pylori evolution and phenotypic diversification in a changing host. Nat Rev Microbiol. 2007;5(6):441–452. doi:10.1038/ nrmicro1658.

22. Baishya J, Wakeman CA. Selective pressures during chronic infection drive microbial competition and cooperation. Npj Biofilms Microbiomes. 2019;5(1):16. doi:10.1038/s41522-019-0089-2.

23. Smith EE, Buckley DG, Wu Z, Saenphimmachak C, Hoffman LR, D'Argenio DA, Miller SI, Ramsey BW, Speert DP, Moskowitz SM, et al. Genetic adaptation by Pseudomonas aeruginosa to the airways of cystic fibrosis patients. Proc Natl Acad Sci USA. 2006;103 (22):8487–8492. doi: 10.1073/pnas.0602138103.

24. Ferreiro A, Crook N, Gasparrini AJ, Dantas G. Multiscale evolutionary dynamics of host-associated microbiomes. Cell. 2018;172(6):1216–1227. doi:10. 1016/j.cell.2018.02.015.

25. Huang S, Jiang S, Huo D, Allaband C, Estaki M, Cantu V, Belda-Ferre P, Vázquez-Baeza Y, Zhu Q, Ma C, et al. Candidate probiotic Lactiplantibacillus plantarum HNU082 rapidly and convergently evolves within human, mice, and zebrafish gut but differentially influences the resident microbiome. Microbiome. 2021;9 (1):151. doi: 10.1186/s40168-021-01102-0.

26. Zuckerkandl E, Pauling L. Evolutionary divergence and convergence in proteins. In: Evol genes proteins. Elsevier; 1965. p. 97–166. doi: 10.1016/B978-1-4832-2734-4.50017-6.

27. Stautz J, Hellmich Y, Fuss MF, Silberberg JM, Devlin JR, Stockbridge RB, Hänelt I. Molecular mechanisms for bacterial potassium homeostasis. J Mol Biol. 2021;433(16):166968. doi:10.1016/j.jmb. 2021.166968.

28. Wang J, Chitsaz F, Derbyshire MK, Gonzales NR, Gwadz M, Lu S, Marchler Gabriele H, Song James S, Thanki N, Yamashita Roxanne A, et al. The conserved domain database in 2023. Nucleic Acids Res. 2022;51 (D1):D384–D388. doi: 10.1093/nar/gkac1096.

29. Anantharaman V, Aravind L. Evolutionary history, structural features and biochemical diversity of the NlpC/P60 superfamily of enzymes. Genome Biol. 2003;4(2):R11. doi:10.1186/gb-2003-4-2-r11.

30. Szollosi D, Rose-Sperling D, Hellmich UA, Stockner T. Comparison of mechanistic transport cycle models of ABC exporters. Biochim Biophys Acta Biomembr. 2018;1860(4):818–832. doi: 10.1016/j.bbamem.2017. 10.028.

31. Li R, Zhu H, Ruan J, Qian W, Fang X, Shi Z, Li Y, Li S, Shan G, Kristiansen K, et al. De Novo assembly of human genomes with massively parallel short read sequencing. Genome Res. 2010;20(2):265–272. doi: 10. 1101/gr.097261.109.

32. Ferrari A, Maggi S, Montanini B, Levante A, Lazzi C, Yamaguchi Y, Rivetti C, Folli C. Identification and first characterization of DinJ-YafQ toxin-antitoxin systems in Lactobacillus species of biotechnological interest. Sci Rep. 2019;9(1):7645. doi:10.1038/s41598-019-44094-6.

33. Levante A, Lazzi C, Vatsellas G, Chatzopoulos D, Dionellis VS, Makrythanasis P, Neviani E, Folli C. Genome sequencing of five Lacticaseibacillus strains and analysis of type I and II toxin-antitoxin system distribution. Microorganisms. 2021;9(3):648. doi:10. 3390/microorganisms9030648.

34. Cai T, Zhao QH, Xiang WL, Zhu L, Rao Y, Tang J. HigBA toxin–antitoxin system of Weissella cibaria is involved in response to the bile salt stress. J Sci Food Agric. 2022;102(14):6749–6756. doi:10.1002/jsfa.12042 .

35. Kocher CD, Dill KA. Darwinian evolution as a dynamical principle. Proc Natl Acad Sci USA. 2023;120(11): e2218390120. doi: 10.1073/pnas.2218390120.

36. Yang Y, Nguyen M, Khetrapal V, Sonnert ND, Martin AL, Chen H, Kriegel MA, Palm NW. Within-host evolution of a gut pathobiont facilitates liver translocation. Nature. 2022;607(7919):563–570. doi:10.1038/s41586-022-04949-x.

37. Key FM, Khadka VD, Romo-González C, Blake KJ, Deng L, Lynn TC, Lee JC, Chiu IM, García-Romero MT, Lieberman TD. On-person adaptive evolution of Staphylococcus aureus during treatment for atopic dermatitis. Cell Host Microbe. 2023;31(4):593–603.e7. doi: 10.1016/j.chom.2023.03.009.

38. Jiang S, Zhang C, Han Z, Ma W, Wang S, Huo D, Cui W, Zhai Q, Huang S, Zhang J. Native microbiome dominates over host factors in shaping the probiotic genetic evolution in the gut. npj Biofilms Microbiomes. 2023;9(1):80. doi:10.1038/s41522-023-00447-8.

39. Markowiak P, K Ś. Effects of probiotics, prebiotics, and synbiotics on human health. Nutrients. 2017;9(9):1021. doi: 10.3390/nu9091021.

40. Thursby E, Juge N. Introduction to the human gut microbiota. Biochemical J. 2017;474(11):1823–1836. doi: 10.1042/bcj20160510.

41. Duar RM, Frese SA, Lin XB, Fernando SC, Burkey TE, Tasseva G, Peterson DA, Blom J, Wenzel CQ, Szymanski CM, et al. Experimental evaluation of host adaptation of lactobacillus reuteri to different vertebrate species. Appl Environ Microbiol. 2017;83(12): e00132–17. doi: 10.1128/AEM.00132-17.

42. Achtman M, Zurth K, Morelli G, Torrea G, Guiyoule A, Carniel E. Yersinia pestis, the cause of plague, is a recently emerged clone of Yersinia pseudotuberculosis. Proc Natl Acad Sci USA. 1999;96(24):14043–14048. doi: 10.1073/pnas.96.24.14043.

43. Zhang J, Wang X, Huo D, Li W, Hu Q, Xu C, Liu S, Li C. Metagenomic approach reveals microbial diversity and predictive microbial metabolic pathways in Yucha, a traditional Li fermented food. Sci Rep. 2016;6 (1):32524. doi: 10.1038/srep32524.

44. Shao Y, Huo D, Peng Q, Pan Y, Jiang S, Liu B, Zhang J. Lactobacillus plantarum HNU082-derived improvements in the intestinal microbiome prevent the development of hyperlipidaemia. Food Funct. 2017;8 (12):4508–4516. doi: 10.1039/c7fo00902j.

45. Zhang Z, Peng Q, Huo D, Jiang S, Ma C, Chang H, Chen K, Li C, Pan Y, Zhang J. Melatonin regulates the neurotransmitter secretion disorder induced by caffeine through the microbiota-gut-brain axis in zebrafish (danio rerio). Front Cell Dev Biol. 2021;9:678190. doi: 10.3389/fcell.2021.678190.

46. Chen S, Zhou Y, Chen Y, Gu J. Fastp: an ultra-fast all-in-one FASTQ preprocessor. Bioinformatics. 2018;34 (17):i884–i890. doi:10.1093/bioinformatics/bty560.

47. Jain C, Lm R-R, Phillippy AM, Konstantinidis KT, Aluru S. High throughput ANI analysis of 90K prokaryotic genomes reveals clear species boundaries. Nat Commun. 2018;9(1):5114. doi: 10.1038/s41467-018-07641-9.

48. Olm MR, Crits-Christoph A, Bouma-Gregson K, Firek BA, Morowitz MJ, Banfield JF. inStrain profiles population microdiversity from metagenomic data and sensitively detects shared microbial strains. Nat Biotechnol. 2021;39(6):727–736. doi:10.1038/s41587-020-00797-0.

49. Hyatt D, Chen GL, Locascio PF, Land ML, Larimer FW, Hauser LJ. Prodigal: prokaryotic gene recognition and translation initiation site identification. BMC Bioinform. 2010;11(1):119. doi: 10.1186/1471-2105-11-119.

50. Langmead B, Salzberg SL. Fast gapped-read alignment with bowtie 2. Nat Methods. 2012;9(4):357–359. doi:10. 1038/nmeth.1923.

51. Kumar S, Stecher G, Li M, Knyaz C, Tamura K. MEGA X: Molecular evolutionary genetics analysis across computing platforms. Mol Biol Evol. 2018;35(6):1547–1549. doi: 10.1093/molbev/msy096.

52. Letunic I, Bork P. Interactive tree of life (iTOL) v5: an online tool for phylogenetic tree display and

annotation. Nucleic Acids Res. 2021;49(W1):W293–W296. doi: 10.1093/nar/gkab301.

53. Deamer D, Akeson M, Branton D. Three decades of nanopore sequencing. Nat Biotechnol. 2016;34(5):518–524. doi:10.1038/nbt.3423.

54. De Coster W, Rademakers R, Alkan C. NanoPack2: population-scale evaluation of long-read sequencing data. Bioinformatics. 2023;39(5):btad311. doi: 10.1093/bioinformatics/btad311.

55. Kolmogorov M, Bickhart DM, Behsaz B, Gurevich A, Rayko M, Shin SB, Kuhn K, Yuan J, Polevikov E, Smith TPL, et al. metaFlye: scalable long-read metagenome assembly using repeat graphs. Nat Methods. 2020;17 (11):1103–1110. doi: 10.1038/s41592-020-00971-x.

56. Vaser R, Sović I, Nagarajan N, M Š. Fast and accurate de novo genome assembly from long uncorrected reads. Genome Res. 2017;27(5):737–746. doi: 10.1101/gr.214270.116.

57. Li H, Birol I. Minimap2: pairwise alignment for nucleotide sequences. Bioinformatics. 2018;34(18):3094–3100. doi: 10.1093/bioinformatics/bty191.

58. Hyatt D, Chen G-L, Pf L, Land ML, Larimer FW, Hauser LJ. Prodigal: prokaryotic gene recognition and translation initiation site identification. BMC Bioinform. 2010;11(1):1–11. doi: 10.1186/1471-2105-11-119.

59. O'Donnell S, Fischer G, Valencia A. MUM&Co: accurate detection of all SV types through whole-genome alignment. Bioinformatics. 2020;36(10):3242–3243. doi: 10.1093/bioinformatics/btaa115.

60. Xie Z, Tang H, Hancock J. ISEScan: automated identification of insertion sequence elements in prokaryotic genomes. Bioinformatics. 2017;33(21):3340–3347. doi: 10.1093/bioinformatics/btx433.

61. Desjardins P, Conklin D. NanoDrop microvolume quantitation of nucleic acids. J Visualized Experiments: JoVE. 2010;2010(45). doi: 10.3791/2565.

62. Lozano-Peral D, Rubio L, Santos I, Gaitan MJ, Viguera E, Martin-de-Las-Heras S. DNA degradation in human teeth exposed to thermal stress. Sci Rep. 2021;11 (1):12118. doi:10.1038/s41598-021-91505-8.

63. Beghini F, McIver LJ, Blanco-Miguez A, Dubois L, Asnicar F, Maharjan S, Mailyan A, Manghi P, Scholz M, Thomas AM, et al. Integrating taxonomic, functional, and strain-level profiling of diverse microbial communities with bioBakery 3. Elife. 2021;10. doi: 10.7554/eLife.65088.

64. Buchfink B, Xie C, Huson DH. Fast and sensitive protein alignment using DIAMOND. Nat Methods. 2015;12(1):59–60. doi:10.1038/nmeth.3176.

65. Huang L, Zhang H, Wu P, Entwistle S, Li X, Yohe T, Yi H, Yang Z, Yin Y. dbCAN-seq: a database of carbohydrate-active enzyme (CAZyme) sequence and annotation. Nucleic Acids Res. 2018;46(D1):D516–D521. doi: 10.1093/nar/gkx894.

66. Li D, Liu CM, Luo R, Sadakane K, Lam TW. MEGAHIT: an ultra-fast single-node solution for large and complex metagenomics assembly via succinct de Bruijn graph. Bioinformatics. 2015;31(10):1674–1676. doi:10.1093/bioinformatics/btv033.

67. Jiang S, Liu A, Ma W, Liu X, Luo P, Zhan M, Zhou X, Chen L, Zhang J. Lactobacillus gasseri CKCC1913 mediated modulation of the gut–liver axis alleviated insulin resistance and liver damage induced by type 2 diabetes. Food Funct. 2023;14(18):8504–8520. doi: 10.1039/d3fo01701j.

68. Guo Q, Wang G, Zheng L, Xue H, Wang R, Fang Y, Zhang J. A WYL domain transcription factor regulates Lactiplantibacillus plantarum intestinal colonization via perceiving c-di-GMP. Nat Commun. 2025;16 (1):2193. doi:10.1038/s41467-025-57581-4.

69. Shannon P, Markiel A, Ozier O, Baliga NS, Wang JT, Ramage D, Amin N, Schwikowski B, Ideker T. Cytoscape: a software environment for integrated models of biomolecular interaction networks. Genome Res. 2003;13(11):2498–2504. doi: 10.1101/gr.1239303.

70. Gu Z, Gu L, Eils R, Schlesner M, Brors B. Circlize implements and enhances circular visualization in R. Bioinformatics. 2014;30(19):2811–2812. doi:10.1093/bioinformatics/btu393.

71. Wickham H ggplo Wiley interdisciplinary reviews: computational statistics. 2011 2. 3(2):180–185. doi: 10.1002/wics.147.

72. Kolde R. Package 'pheatmap'. R Package. 2015;1(7):790. doi: 10.32614/CRAN.package.pheatmap.

73. Dixon P. VEGAN, a package of R functions for community ecology. J Veg Sci. 2003;14(6):927–930. doi: 10.1111/j.1654-1103.2003.tb02228.x.

74. Palarea-Albaladejo J, Martín-Fernández JA. zCompositions — R package for multivariate imputation of left-censored data under a compositional approach. Chemom Intell Lab Syst. 2015;143:85–96. doi: 10.1016/j.chemolab.2015.02.019.

75. Zhang J. Package 'spaa'. R package version. 2013;1(1). doi: 10.32614/CRAN.package.spaa.

76. Yuan MM, Guo X, Wu L, Zhang Y, Xiao N, Ning D, Shi Z, Zhou X, Wu L, Yang Y, et al. Climate warming enhances microbial network complexity and stability. Nat Clim Change. 2021;11(4):343–348. doi: 10.1038/s41558-021-00989-9.

77. Kelley LA, Mezulis S, Yates CM, Wass MN, Sternberg MJ. The Phyre2 web portal for protein modeling, prediction and analysis. Nat Protoc. 2015;10(6):845–858. doi:10.1038/nprot.2015.053.

78. Vilar S, Cozza G, Moro S. Medicinal chemistry and the molecular operating environment (MOE): application of QSAR and molecular docking to drug discovery. Curr Top Med Chem. 2008;8(18):1555–1572. doi: 10.2174/156802608786786624.